PAPER

Check for updates

An all-solid-state potentiometric microsensor for real-time monitoring of the calcification process by *Bacillus subtilis* biofilms†

Jiabin Wang,[ab] Jiawang Ding (iD) *[abcd] and Wei Qin (iD) [abcd]

Bacillus subtilis, as a bacterium with wide-ranging applications, has been explored for CO_2 sequestration using intracellular or extracellular carbonic anhydrase (CA). However, noninvasive, real-time monitoring of CA-mediated calcium carbonate precipitation processes is scarce, especially for bacteria in seawater. We report here the use of a carbon nanotube fiber-filled glass micropipette for preparing mechanically robust ion-selective microelectrodes for *in situ* ion sensing. Hydrophobic carbon nanotube fibers with remarkable electrical and mechanical properties can act not only as a transduction layer but also as a self-supporting material. As a model, an all-solid calcium ion-selective microelectrode (Ca^{2+}-ISμE) with a size of 20 μm was designed. The Ca^{2+}-ISμE shows a Nernstian response to Ca^{2+} in 0.5 M sodium chloride within the range of 1.0×10^{-6}–1.0×10^{-2} M, and the detection limit is 4.0×10^{-7} M. The proposed microsensor allows for *in situ*, real-time monitoring of the calcification process by *Bacillus subtilis* biofilms. This work provides a simple and versatile tool to monitor biomineralization processes and reveal carbon concentration and sequestration mechanisms.

Introduction

Microbial-mediated carbonate precipitation is one kind of biomineralization that has been widely used in soil remediation, building restoration, corrosion protection, and CO_2 sequestration.[1–4] Recently it has been reported that at least 200 species of microbes have been found able to induce calcium carbonate precipitation.[5] Among these microorganisms, *Bacillus subtilis* is a bacterium commonly used in industry and research and has been widely distributed in water, soil, and air. Carbonic anhydrases (CAs) are metalloenzymes found in this kind of bacterium and play a key role in the bacteria-mediated calcium carbonate deposition process. Extracellular or intracellular CAs can reversibly catalyze the hydration of carbon dioxide, release carbonate or bicarbonate ions to bind

cations (*e.g.*, Ca^{2+}) and ultimately cause the precipitation of $CaCO_3$. Thus, this bacterium has gained widespread attention for its potential role in carbon dioxide (CO_2) sequestration. Previous research has shown that the precipitation process is controlled by several factors, including pH, the amount of CAs, concentration of calcium ions, and presence of nucleation sites.[6] Much progress has been made in recent decades in better understanding this complex process by using various techniques for chemical and morphology characterization. However, the presence of a high electrolyte background for marine and biological environments poses a challenge for sensitive measurements. Moreover, the understanding of biomineralization processes is still hindered by the heterogeneity in biofilm structure and associated spatial variation in cell density. So far, *Bacillus subtilis* biofilm-induced calcification in marine environments has never been explored. Therefore, techniques that can achieve non-invasive, *in situ* and real-time detection of this process are still highly required due to the dynamic biomineralization process.

Microsensors based on polymeric membrane ion-selective electrodes (ISμEs) have attractive features such as a fast response time, low detection limit, broad dynamic response range and minimal sample perturbation. These potentiometric microelectrodes have become an indispensable tool for *in vitro* and *in vivo* ion sensing and allow us to monitor ion concentrations or ion fluxes in various fields, including biological analysis,[7–9] environmental

[a] CAS Key Laboratory of Coastal Environmental Processes and Ecological Remediation, Shandong Key Laboratory of Coastal Environmental Processes, YICCAS, Yantai Institute of Coastal Zone Research (YIC), Chinese Academy of Sciences (CAS), Yantai 264003, Shandong, P. R. China. E-mail: jwding@yic.ac.cn
[b] University of Chinese Academy of Sciences, Beijing 100049, P. R. China
[c] Center for Ocean Mega-Science, Chinese Academy of Sciences Center for Ocean Mega-Science, Chinese Academy of Sciences, Qingdao 266071, Shandong, P. R. China
[d] Laboratory for Marine Biology and Biotechnology, Pilot National Laboratory for Marine Science and Technology (Qingdao), Qingdao 266237, Shandong, P. R. China
† Electronic supplementary information (ESI) available. See DOI: https://doi.org/10.1039/d3sd00017f

monitoring,[10,11] and corrosion process investigation.[12,13] Moreover, the combination of potentiometric microsensors with scanning electrochemical microscopy allowed the direct high-resolution visualization of local variations in the surface activity of specific ions.[14] Traditional microelectrodes with liquid-inner filling solutions still face problems such as easy leakage, short lifetimes and low sensitivity. Therefore, all-solid-state potentiometric microelectrodes with easy preparation, low detection limit and good stability are considered as a promising alternative to traditional internal solution ion-selective microelectrodes. To date, many classes of materials, including conducting polymers and carbon or noble metal-based materials, have been integrated into all-solid-state potentiometric sensors to improve their sensitivity, stability and reproducibility.[15,16] Carbon nanotubes with inherent hydrophobicity, good electrical conductivity, and a certain specific capacitance have been used as ion-to-electron transduction layers[17,18] in solid-state ion-selective electrodes for anions,[19,20] cations,[18,21] and small molecules.[22] Primitive and functionalized carbon nanotubes can not only eliminate the unwanted water layer between the ion-selective membrane and the electrode substrate but also show significant advantages in terms of ion-to-electron transduction.[23] In recent years, fibers of aligned CNTs that can well preserve the characteristics of individual CNTs have been prepared and utilized as electrode materials in many areas, such as electronics, energy storage, and health care.[24] CNT fiber microelectrodes were demonstrated to have high chemical stability and mechanical strength, excellent electroactivity, and resistance to fouling.[25,26] However, currently reported electrochemical microsensors focus primarily on amperometric detection of redox species. The in-depth study and use of carbon nanotube fiber-based materials in all-solid-state potential microsensors is still unexplored.

In this study, a facile protocol for preparing an all-solid-state ion-selective microelectrode (ISμE) based on carbon nanotube fibers is proposed for the first time. Carbon nanotube fibers not only serve as electrode substrates but can also be used as an ion-to-electron transduction layer to improve the stability of electrode potential. To measure the process of biomineralization in seawater, an all-solid calcium ion-selective microelectrode (Ca^{2+}-ISμE) was prepared. The proposed carbon nanotube fiber-based microelectrodes have high sensitivity, good stability and biocompatibility and were successfully applied to sense *Bacillus subtilis* biofilm-induced calcification *in situ* and in real time.

Materials and methods

Chemicals and materials

ETH 129 (Ca^{2+} ionophore II), 2-nitrophenyl octyl ether (*o*-NPOE), high molecular weight polyvinyl chloride (PVC), tetradodecylammonium tetrakis(4-chlorophenyl)borate (selectophore, ETH 500) and NaCl (99.999%) were purchased from Sigma-Aldrich. 3140 RTV silicone rubber was obtained

from Dow Corning (Korea). The lipophilic cation-exchanger sodium tetrakis[3,5-bis(trifluoromethyl)phenyl]borate (NaTFPB) was purchased from Alfa Aesar. Carbon nanotube fibers with a diameter of 10–20 μm were purchased from Jiacai Technology Co., Ltd. (Chengdu, China). Acetazolamide was obtained from Macklin Biochemical Technology Co., Ltd. (Shanghai, China). *N*-Dimethyltrimethylsilylamine was obtained from MREDA Technology Co., Ltd. (Beijing, China). All other chemicals were of analytical reagent grade. Deionized water (18.2 MΩ specific resistance) used throughout was obtained with a Synergy® UV water purification system.

Apparatus and measurements

Potentiometric measurements were performed at room temperature using a Model PXSJ-216 digital ion analyser (Shanghai, China). The Ca^{2+}-ISμE and Ag/AgCl/3 M KCl microelectrodes were used as the indicator and reference electrodes, respectively. The reference electrode with a size of 20 μm was prepared as described before with modification.[27] Briefly, 2% agar hot solution was drawn into a micropipette by its capillarity. After cooling, 3 M KCl solution was injected into the micropipette. Then, Ag/AgCl wire was inserted into the capillary tube. Ca^{2+}-ISμE was conditioned in a 10^{-3} M CaCl$_2$ solution overnight before potentiometric measurements. The ion activities were calculated by the Debye–Hückel approximation[28] and the potentiometric values were corrected for liquid junction potentials with the Henderson equation.[29] Electrochemical impedance and cyclic voltammetry measurements were carried out using a CHI-660E electrochemical workstation (Shanghai, China) using conventional three electrode configurations. Cyclic voltammetry was performed in a 5 mM K$_4$[Fe(CN)$_6$] solution containing 0.1 M KCl. Electrochemical impedance measurements were carried out in 0.1 M KCl at open circuit potential with an excitation amplitude of 100 mV and a frequency range of 0.1 Hz–100 kHz.

Fabrication of the Ca^{2+}-selective microsensor

The Ca^{2+}-selective membrane components (total of 360 mg) containing 2.3% calcium ionophore II, 2.2% NaTFPB, 5.0% 3140 RTV silicone rubber, 1.0% ETH500, 29.8% PVC, and 59.7% *o*-NPOE were dissolved in 3.6 mL tetrahydrofuran. The micropipettes were fabricated with a micropipette puller (P-1000, Sutter Instruments) using a cleaned borosilicate glass capillary (1.0 mm o.d., 0.589 mm i.d., 10.0 cm length, Sutter). The micropipettes with a tip of 20 μm were immersed in *N*-dimethyltrimethylsilylamine for silanization and baked at 150 °C for 3 h in a vacuum drying box. Carbon nanotube fibers were fixed on the end of a copper wire with graphene-based conductive glue (Nanjing XFNANO Materials Tech Co., Ltd). A carbon nanotube fiber-filled glass micropipette was used to prepare the microsensor by dip coating in the ion-selective membrane cocktail (Fig. 1A). Each microsensor was
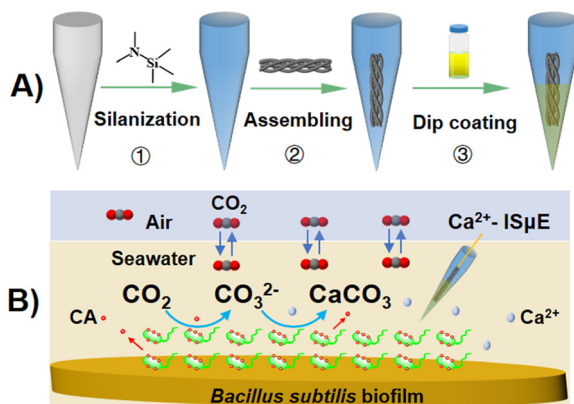
Fig. 1 (A) Schematic diagram of the preparation process of CNT fiber/Ca^{2+}-ISμE. (B) Schematic diagram of monitoring the dynamic changes in Ca^{2+} concentration above the biofilm using Ca^{2+}-ISμE.

checked by optical microscopy to ensure the attachment of the polymeric membrane.

Preparation and characterization of membrane biofilms

Bacillus subtilis maintained in Luria–Bertani (LB) medium was purchased from the Marine Microbial Preservation and Management Center (Xiamen, China). *Bacillus subtilis* (1A14617) was isolated from mangrove sediments in Fujian, China. The composition of the LB medium was as follows: 10 g L^{-1} tryptone, 5 g L^{-1} yeast extract, 10 g L^{-1} sodium chloride, and 15 g L^{-1} agar (for gel plates). After being cultured at 30 °C for 1 day, *Bacillus subtilis* in the logarithmic growth stage was used to prepare the biofilm samples. After centrifugation and washing in saline (0.9% NaCl), a 1.0 mL aliquot of suspended bacteria was pipetted and plated over a sterile polycarbonate membrane (0.2 μm pore size) on a nutrient-containing agar plate. The bacteria-containing membrane/agar plate was later incubated at 30 °C for 72 h. For potentiometric measurements, the membrane biofilm was carefully removed from the agar plate using a tweezer and affixed at the bottom of a small Petri dish with double-sided tape. *Bacillus subtilis* biofilms were incubated in pH = 8.0 Tris–HCl buffer with 0.01 M calcium ions. The incubation times were 0.5 and 12 h, respectively. For scanning electron microscopy (SEM) analysis, the biofilms were fixed overnight at 4 °C with 2.5% glutaraldehyde and 1% paraformaldehyde in 0.1 M sodium cacodylate buffer. After fixation, the biofilm was rinsed several times with buffer solution. Then, the biofilm was dehydrated in an ethanol concentration gradient (10%, 30%, 50%, 70%, 90%, 100%) for 15 min for each gradient. The prepared samples were kept dry prior to imaging.

Real-time monitoring of the calcification process

To explore *Bacillus subtilis* biofilm-induced calcification in real time, biofilms were prepared as described above. In the presence of Ca^{2+}, the rapid interconversion of CO_2 and water by the biofilm can release carbonate or bicarbonate ions to

precipitate $CaCO_3$. As such, the precipitation process can be detected by using the proposed Ca^{2+}-ISμE placed above the biofilm (Fig. 1B). The whole measuring system was controlled by a micromanipulator (Narishige, Japan) and maintained in a Faraday cage to reduce external electromagnetic interferences.

Results and discussion

Fabrication and characteristics of the microelectrodes

Carbon dioxide (CO_2), as one of the most important gases in the environment and also a dominant greenhouse gas, can lead to global warming and climate change. In recent years, bio-precipitation of carbon through microbial enzymes has been explored for CO_2 sequestration.[30] The hydration of CO_2 is a rate-limiting step in the process of its sequestration, which can be accelerated by microbial enzymes especially carbonic anhydrase (CA). In this study, CO_2 biocatalytic convertion processes through bacterial CA were measured in a real-time manner. As an example, *Bacillus subtilis* biofilm-induced calcification in marine environments was explored (Fig. 1). To achieve real-time monitoring of the biofilm-induced calcification process, a general strategy for the preparation of a robust all-solid-state potentiometric microsensor was designed. CNT fiber-filled glass micropipettes were prepared as described in Fig. 1A. The proposed configuration is able to entrap the ion-selective membrane and improve the robustness of the microelectrode. CNT fibers can provide a 3D carbon scaffold possessing excellent mechanical strength, large surface areas, and high conductivity and can be an ideal support for fabricating microsensors. Unlike previous microsensor designs, where gold wires and/or carbon fibers as an excellent microelectrode material were coated with
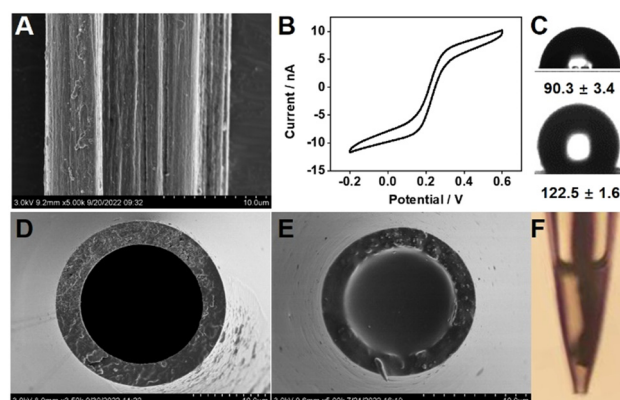

Fig. 2 (A) SEM image of a CNT fiber. (B) Cyclic voltammogram of the CNT fiber in a 5 mM $K_4[Fe(CN)_6]$ solution containing 0.1 M KCl. The scan rate was 50 mV s^{-1}. (C) The contact angles measured on the surface of the silanized glass (top) and the carbon nanotube film (bottom). (D) and (E) SEM images of the glass micropipettes before and after adsorption of the calcium ion-selective membrane cocktail. (F) Micrograph of CNT fiber/Ca^{2+}-ISμE. The digital photomicrographs were collected at 100× optical magnification.

conducting polymers, the CNT fibers can serve as not only an electrode substrate but also a solid-contact ion-to-electron transducer.

The CNT fiber was made of carbon nanotubes grown naturally in a line. Scanning electron microscopy (SEM) images show that the surface of the CNT fiber has a uniform striped pattern, reflecting the aligned filament of the outer surface of the CNTs (Fig. 2A). The CV response was collected at 50 mV s^{-1} in a 5 mM $K_4[Fe(CN)_6]$ solution containing 0.1 M KCl. As shown in Fig. 2B, due to the electrode's small size and fast radial diffusion, the proposed CNT fiber microelectrode shows a sigmoidal steady state-limiting current with a magnitude of 10 nA. Note that a charging current can be noticed. The limiting current (I_{lim}) of the microelectrode is given by $I_{lim} = 4nFDCr$, where n refers to the number of electrons transferred per redox event, F is the Faraday constant, D is the diffusion coefficient, C is the bulk concentration of the redox molecules, and r is the electrode radius.[31] The r of this electrode is calculated to be 17 μm, which is consistent with that measured by SEM imaging.

To prevent aqueous layer formation under the ion-selective membrane and improve the reproducibility of the solid-contact ion-selective electrode, highly hydrophobic materials such as perfluorinated alkanoate side chain-functionalized poly(3,4-ethylenedioxythiophene) (PEDOTF),[32] PEDOT-C$_{14}$,[33] and redox molecule-functionalized carbon nanotubes[34] have been used. The properties of the CNT fibers were studied by contact angle (CA) analysis (Fig. 2C). The CNT fiber surface exhibited hydrophobic behavior with a contact angle of 122.5° ± 1.5° (n = 3), which can prevent the detachment of the ion-selective membrane and the accumulation of an aqueous layer.[33] Moreover, glass micropipettes were silanized to promote adhesion with the hydrophobic ion-selective membrane. The measured CA was 90.3° ± 3.4° (n = 3). A compact film with strong substrate adhesion is the premise of designing a robust potentiometric microsensor. To further improve the adhesion of the PVC to the carbon nanotube fiber, 3140 RTV silicone rubber was incorporated into the membrane cocktail. Compared to PVC, the silicone rubber film retains its viscoelastic properties, which makes the film sticky and enables strong adhesion to the carbon nanotube fiber. The presence of silicone rubber may also reduce the water uptake of the membranes, which is beneficial to preventing the formation of water layers in all-solid-state ion-selective electrodes.[35] Moreover, silicone rubber was proven to have an antifouling ability,[36] which could enhance its biocompatibility and/or environmental compatibility. As shown in Fig. 2D–F, the tip of the capillary glass appears flat and smooth. More importantly, the ion-selective polymeric film evenly and completely fills the cavity of the microelectrode tip. Further observation by optical microscopy showed that the tips of the carbon nanotube fibres are uniformly coated by a polymeric film, which lays the foundation for good potentiometric performance.
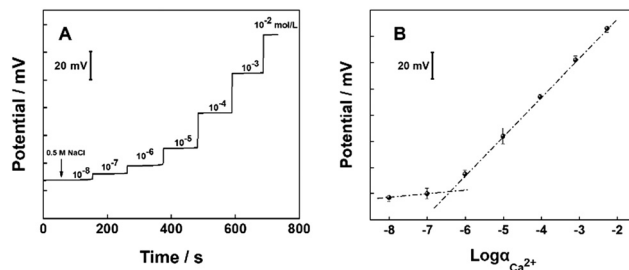

Fig. 3 (A) Potentiometric responses of the CNT fiber/Ca^{2+}-ISμE in 0.5 M NaCl. (B) Calibration curve of the CNT fiber/Ca^{2+}-ISμE. Error bars represent the standard deviation for three measurements.

Potentiometric performance of Ca^{2+}-ISμE

In our study, the capacity of *Bacillus subtilis*, which was isolated from marine sediment, to form biomineralized films on substrate materials was investigated. Therefore, the potentiometric response of Ca^{2+}-ISμE was measured at calcium ion concentrations ranging from 1.0×10^{-2} to 1.0×10^{-8} M in 0.5 M NaCl. The potential response trace of Ca^{2+}-ISμE and the corresponding calibration curve are given. As shown in Fig. 3A and B, the proposed Ca^{2+}-ISμE exhibits a linear response in the concentration range of 1.0×10^{-6} to 1.0×10^{-2} with a Nernstian slope of 27.9 ± 1.2 mV per decade (n = 3). The detection limit was calculated to be 4.0×10^{-7} M based on the intersection of the two slope lines.

Electrochemical impedance analysis of the CNT fiber and CNT fiber/Ca^{2+}-ISμE is shown in Fig. 4A. The semicircle in the high-frequency region depends on the impedance of the ion-selective membrane and the impedance of the conductive
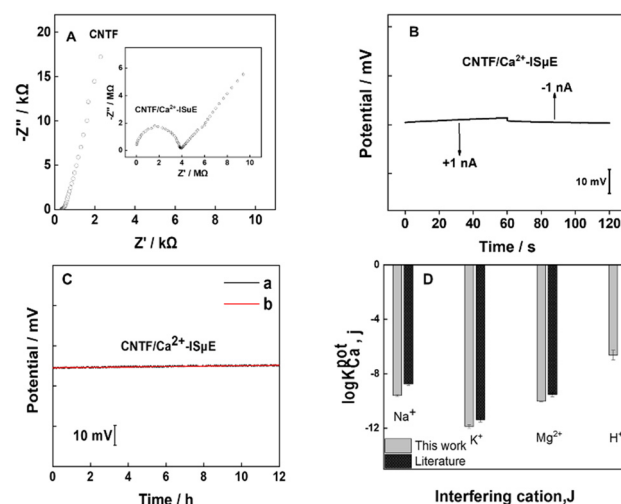

Fig. 4 (A) Electrochemical impedance spectrum for the carbon nanotube fibre. The inset shows the impedance spectrum for CNT fiber/Ca^{2+}-ISμE. (B) Chronopotentiogram for the CNT fiber/Ca^{2+}-ISμE electrodes recorded in 10^{-1} M CaCl$_2$. The applied currents were ±1 nA for 60 s. (C) Long-term stability of the CNT fiber/Ca^{2+}-ISμE. (a) The raw potential response; (b) the linear fit of the raw data. (D) Selectivity coefficient for the Ca^{2+}-selective membrane and a comparison with literature data.[42]

substrate.[37] In the high-frequency region, the CNT fiber microelectrode shows a capacitance curve close to 90°, indicating rapid charge transfer between the electrode interface and the electrolyte solution. As reported previously, potential drift can affect the accuracy and stability of signal recording, which is related to the properties of the solid transduction layer.[38] Therefore, we investigated the short-term and long-term stability of Ca^{2+}-ISμE (Fig. 4B and C). The short-term stability of Ca^{2+}-ISμE was tested using chronopotentiometry with a constant current of ±1 nA for 60 s in 0.1 M CaCl$_2$.[39] The potential drift of Ca^{2+}-ISμE was calculated as 29.9 ± 0.7 μV s^{-1} ($n = 3$), which is lower than that of a micropipette ion-selective electrode using PEDOT nanowires as an ion-to-electron transducer.[40] The long-term stability of Ca^{2+}-ISμE was tested for 12 h in 0.1 M CaCl$_2$. The results are shown in Fig. 4C, where the black line represents the raw data and the red line is the linear fit of the raw data. The potential drift of Ca^{2+}-ISμE was calculated to be 21 ± 6.7 μV h^{-1} ($n = 3$). The high stability of the electrode is probably due to the hydrophobic CNTs, which can not only provide effective ion-to-electron transduction but also prevent the accumulation of an aqueous layer.

Previous research shows that silicone rubber-based membranes may lead to a slow and noisy response in part due to their high electrical resistance. In our work, ETH 500 as one kind of ionic liquid was used to decrease the membrane resistance. Moreover, the amount of silicone rubber incorporated into the cocktail was optimized. Experiments show that the presence of 5% silicone rubber can give a counterbalance between the high viscoelastic properties and low resistance of the membrane. The selectivity coefficients of the Ca^{2+}-selective membrane towards interfering ions were determined by the separate solution method.[41] As shown in Fig. 4D, the results are consistent with values reported in the literature,[42] which indicates that the addition of silicone rubber (5%) to the membrane component will not affect the selectivity of the Ca^{2+}-ISM for other interfering ions. The selectivity coefficient toward hydrogen ions is log$K_{Ca,H}^{pot}$ = −6.6, which indicates that the Ca^{2+}-ISM is insensitive to the sample pH. Therefore, the proposed Ca^{2+}-ISμE could be used for the detection of the dynamics of Ca^{2+} above the biofilm. All these results indicated that the proposed microsensor with high sensitivity and good stability can be a good candidate for *in situ*, real-time monitoring of calcification processes by *Bacillus subtilis* biofilms.

Real-time determination of biofilm-induced calcification processes

To shed light on biofilm-induced calcium carbonate mineralization, the morphology of the biofilms was characterized. With Ca^{2+} ions being adsorbed onto the negatively charged surface of the bacteria, nucleation sites are provided for the deposition of mineralisation products. SEM images reveal that *Bacillus subtilis*-mediated carbonate
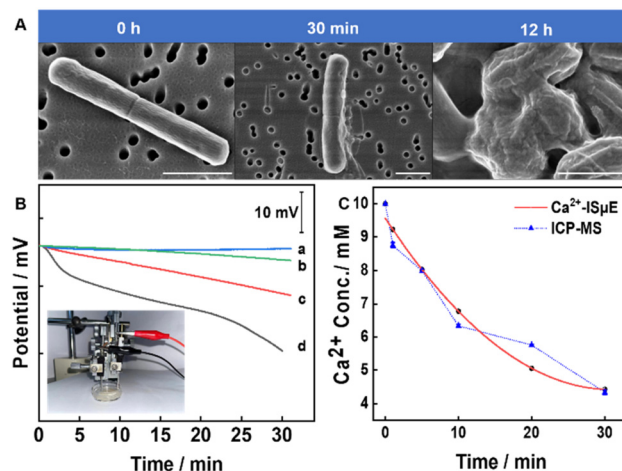

Fig. 5 (A) SEM images of biofilms exposed to buffer solution without calcium and with calcium (10 mM) at different times (30 min, 12 h). Scale bar: 1 μm. (B) Real-time potential response of the Ca^{2+}-ISμE at 200 μm above the biofilm during exposure to 10^{-2} M Ca^{2+} in the presence of acetazolamide (1.5 mg mL^{-1}) (b), 10^{-2} M Ca^{2+} (c), and 10^{-2} M Ca^{2+} in the presence of 10^{-2} M NaHCO$_3$ solution (d). A control experiment was carried out without a biofilm (a). The inset shows the photograph of the setup for *in situ* detection of the calcification process by *Bacillus subtilis* biofilms (an enlarged image of the setup can be found in Fig. S1†). (C) The change in calcium ion activity at 200 μm above the biofilm obtained by Ca^{2+}-ISμE and ICP-MS.

precipitation does exist and is enhanced with incubation time (Fig. 5A). Indeed, without calcium buffer solution, the bacterial morphology exhibits a smooth, three-dimensional structure. After 30 min of incubation in buffer solution containing calcium ions, there was a slight calcification of the surface morphology of the bacteria. As the incubation time increased, calcification of the bacterial surface became more obvious.

Although the formation and apparent morphological changes of CaCO$_3$ on biofilms were observed under scanning electron microscopy, real-time calcium ion change rates are not readily observable. The rate of change in calcium ions can directly characterize the amount of CaCO$_3$ produced and is an important indicator of the calcification process. To measure the change rate of Ca^{2+} during the calcification of the *Bacillus subtilis* biofilm, the Ca^{2+}-ISμE and Ag/AgCl/3 M KCl microelectrode were used as the indicator and reference electrode, respectively. During the test, the microsensor was placed at 200 μm above the biofilm. The movement of the electrode was precisely controlled by the micromanipulator (inset in Fig. 5B). According to the potential curve shown in Fig. 5B, the rate of change in calcium ions gradually accelerates as the concentration of carbon dioxide increases. During the calcification process, CA plays an essential role in inorganic carbon acquisition. As the partial pressure of CO$_2$ increases, the rate of change in calcium ions becomes faster in the first half hour, which indicates that CA can efficiently and rapidly catalyse the deposition reaction. It should be noted that the activity of CA can be affected by pH. At moderate (pH = 7) to highly alkaline

pH, the bicarbonate ions generated were readily deprotonated to form carbonate ions, which allows the build-up to a high enough supersaturation and formation of precipitates of calcium carbonate in the presence of calcium ions.

To better understand the role of CAs in *Bacillus subtilis* biofilms, acetazolamide (ACZ), a carbonic anhydrase inhibitor, was added to the incubation buffer.[43] In the presence of ACZ (Fig. 5B, b), the change rate of calcium ions was significantly slower, which indicates that CA is essential in catalysing the hydration of carbon dioxide to induce biomineralization. As shown in Fig. 5C, the changes in calcium ions measured using Ca^{2+}-ISμE were comparable with the data obtained by inductively coupled plasma-mass spectrometry (ICP-MS). It should be noted that the potentiometric measurements were minimally affected by biofouling in this relatively short period of time.[44] Due to the biofilm inhomogeneity (as indicated in Fig. S2†), the proposed potentiometric method has potential for in-depth studies of microbial-mediated carbonate precipitation. More importantly, the dynamic biomineralization process can be measured in a non-invasive, *in situ* and real-time manner.

Conclusions

This research illustrates a general method for preparing an all-solid-state potentiometric microsensor. Owing to their electrochemical and hydrophobic properties, CNT fibers were explored for designing ion-selective microelectrodes for the first time. CNT fibers serving as both a self-supporting substrate and an ion-to-electron transducer can simplify the preparation procedures and improve the performance of the microsensor. As a model, Ca^{2+}-ISμE with high sensitivity, good stability and reproducibility is demonstrated. The proposed microelectrodes showed excellent performance for the real-time analysis of Ca^{2+} during *Bacillus subtilis* biofilm-induced calcification processes. This simple and reproducible preparation method is general and can be used to prepare other microsensors by using different ion-selective membranes. It is anticipated that this method will be useful for tracing dynamic biomineralization processes and designing potentiometric ion sensors.[45]

Conflicts of interest

There are no conflicts to declare.

Acknowledgements

Notes and references

1 N. Guo, Y. Wang, X. Hui, Q. Zhao, Z. Zeng, S. Pan, Z. Guo, Y. Yin and T. Liu, *J. Mater. Sci. Technol.*, 2021, **7**, 82–90.

2 S. M. Frailey, J. Damico and H. E. Leetaru, *Energy Procedia*, 2011, **4**, 5487.

3 A. C. Mitchell, A. J. Phillips, R. Hiebert, R. Gerlach, L. H. Spangler and A. B. Cunningham, *Int. J. Greenhouse Gas Control*, 2009, **3**, 90–99.

4 C. Rodriguez-Navarro, F. Jroundi, M. Schiro, E. Ruiz-Agudo and M. T. Gonzalez-Munoz, *Appl. Environ. Microbiol.*, 2012, **78**, 4017–4029.

5 X. Li, D. L. Chopp, W. A. Russin, P. T. Brannon, M. R. Parsek and A. I. Packman, *Appl. Environ. Microbiol.*, 2015, **81**, 7403–7410.

6 G. Okwadha and J. Li, *Chemosphere*, 2010, **81**, 1143–1148.

7 J. Church, S. M. Armas, P. K. Patel, K. Chumbimuni-Torres and W. H. Lee, *Electroanalysis*, 2018, **30**, 626–632.

8 J. Hao, T. Xiao, F. Wu, P. Yu and L. Mao, *Anal. Chem.*, 2016, **88**, 11238–11243.

9 G. Zhao, R. Liang, F. Wang, J. Ding and W. Qin, *Sens. Actuators, B*, 2019, **279**, 369–373.

10 D. Harris, J. Ganesh Ummadi, A. R. Thurber, Y. Allau, C. Verba, F. Colwell, M. E. Torres and D. Koley, *Analyst*, 2016, **10**, 2887–2895.

11 G. Zhao, J. Ding and W. Qin, *Anal. Chim. Acta*, 2019, **1073**, 39–44.

12 G. Varga, L. Nagy, J. Izquierdo, I. Bitter and G. Nagy, *Anal. Lett.*, 2011, **44**, 2876–2886.

13 D. Filotás, B. M. Fernández-Pérez, L. Nagy, G. Nagy and R. M. Souto, *Sens. Actuators, B*, 2019, **296**, 126625.

14 M. Etienne, A. Schulte, S. Mann, G. Jordan, I. D. Dietzel and W. Schuhmann, *Anal. Chem.*, 2004, **76**, 3682–3688.

15 C. R. Rousseau and P. Bühlmann, *TrAC, Trends Anal. Chem.*, 2021, **140**, 116277.

16 J. Zhai, D. Yuan and X. Xie, *Sens. Diagn.*, 2022, **1**, 213–221.

17 E. J. Parra, G. A. Crespo, J. Riu, A. Ruiz and F. X. Rius, *Analyst*, 2009, **134**, 1905–1910.

18 L. A. Hussein, N. Magdy and H. Z. Yamani, *Sens. Actuators, B*, 2017, **247**, 436–444.

19 D. Yuan, A. H. C. Anthis, M. Ghahraman Afshar, N. Pankratova, M. Cuartero, G. A. Crespo and E. Bakker, *Anal. Chem.*, 2015, **87**, 8640–8645.

20 K. Pietrzak and C. Wardak, *Sens. Actuators, B*, 2021, **348**, 130720.

21 M. Debosz, J. Kozma, R. Porada, M. Wieczorek, J. Paluch, R. E. Gyurcsányi, J. Migdalski and P. Koscielniak, *Talanta*, 2021, **232**, 122491.

22 H. Abdrabboh, A. E. Amr, A. A. Almehizia and A. H. Kamel, *Polymer*, 2021, **13**, 1192.

23 Y. Liu, Y. Liu, R. Yan, Y. Gao and P. Wang, *Electrochim. Acta*, 2020, **331**, 135370.

24 F. Wang, S. Zhao, Q. Jiang, R. Li, Y. Zhao, Y. Huang, X. Wu, B. Wang and R. Zhang, *Cell Rep. Phys. Sci.*, 2022, **3**, 100989.

25 F. Vitale, S. R. Summerson, B. Aazhang, C. Kemere and M. Pasquali, *ACS Nano*, 2015, **9**, 4465–4474.

26 J. Wang, R. P. Deo, P. Poulin and M. Mangey, *J. Am. Chem. Soc.*, 2003, **125**, 14706–14707.

27 T. Kitade, K. Kitamura, S. Takegami, Y. Miyata, M. Nagatomo, T. Sakaguchi and M. Furukawa, *Anal. Sci.*, 2005, **21**, 907–912.

28 I. Uemasu and Y. Umezawa, *Anal. Chem.*, 1983, **55**, 386–388.

29 A. J. Brad and L. R. Faulkner, *Electrochemical Methods Fundamentals and Applications*, John Wiley&Sons, Inc., New York, 2nd edn, 2001.

30 V. K. Nathan and P. Ammini, *Water, Air, Soil Pollut.*, 2019, **230**, 192.

31 X. Zhang and B. Ogorevc, *Anal. Chem.*, 1998, **70**, 1646–1651.

32 S. Papp, M. Bojtár, R. E. Gyurcsányi and T. Lindfors, *Anal. Chem.*, 2019, **91**, 9111–9118.

33 M. Guzinski, J. M. Jarvis, P. D'Orazio, A. Izadyar, B. D. Pendley and E. Lindner, *Anal. Chem.*, 2017, **89**, 8468–8475.

34 J. Kozma, S. Papp and R. E. Gyurcsányi, *Anal. Chem.*, 2022, **94**, 8249–8257.

35 F. Sundfors, T. Lindfors, L. Höfler, R. Bereczki and R. E. Gyurcsányi, *Anal. Chem.*, 2009, **81**, 5925–5934.

36 J. Thomas, S. B. Choi, R. Fjeldheim and P. Boudjouk, *Biofouling*, 2004, **20**, 227–236.

37 J. Li, T. Yin and W. Qin, *Sens. Actuators, B*, 2017, **239**, 438–446.

38 J. M. Jarvis, M. Guzinski, B. D. Pendley and E. Lindner, *J. Solid State Electrochem.*, 2016, **20**, 3033–3041.

39 J. Bobacka, *Anal. Chem.*, 1999, **71**, 4932–4937.

40 G. Gyetvai, S. Sundblom, L. Nagy, A. Ivaska and G. Nagy, *Electroanalysis*, 2007, **19**, 1116–1122.

41 E. Bakker, E. Pretsch and P. Bühlmann, *Anal. Chem.*, 2000, **72**, 1127–1133.

42 T. Jiang, L. Qi and W. Qin, *Anal. Chem.*, 2019, **91**, 13268–13274.

43 J. M. Mercado, T. Ramírez and D. Cortés, *J. Phycol.*, 2009, **45**, 8–15.

44 J. Kuhlmann, L. C. Dzugan and W. R. Heineman, *Electroanalysis*, 2012, **24**, 1732–1738.

45 J. Xu, Z. Zhang, S. Gan, H. Gao, H. Kong, Z. Song, X. Ge, Y. Bao and L. Niu, *ACS Sens.*, 2020, **5**, 2834–2842.